processes

Article

Model for the Failure Prediction Mechanism of In-Service Pipelines Based on IoT Technology

Xiaotian Zhang and Xingbing Xie *

College of Geophysics and Petroleum Resources, Yangtze University, Wuhan 430100, China
* Correspondence: 500052@yangtzeu.edu.cn

Abstract: With the rapid increase in pipeline mileage in China, the accurate prediction of corrosion issues in in-service pipelines has become crucial for ensuring safe pipeline operation. Traditional pipeline leakage monitoring methods are significantly limited by human factors and equipment precision, making it challenging to predict and identify leakage points accurately. Therefore, aligned with the trend of intelligent pipeline development, this study aims to construct a failure pressure prediction mechanism model for corroded pipelines based on IoT technology. This model leverages intelligent sensing and prediction to assess the safety status of corroded pipeline sections. Ultrasonic phased array technology detects specific corrosion points and detailed defect parameters within pipeline sections. The parameters are then utilized in the Simdroid domestic finite element analysis model to simulate the ultimate burst pressure of the pipeline. A single-variable approach is employed to analyze the sensitivity of different parameters to the pipeline's ultimate burst pressure, with the minimum burst pressure point of multi-point corroded sections selected as the overall segment failure pressure. Finite element simulation data are integrated into a neural network database to predict the pipeline failure pressure. The real-time operational data of the pipeline are monitored using negative-pressure wave sensing. The operational pressure of the corroded points is compared with the algorithm-predicted failure pressure; if the values approach a critical threshold, an alarm is triggered. Moreover, the remote control terminals evaluate the pipeline's self-rescue time, providing a buffer for pipeline leakage self-rescue. The failure prediction mechanism model for in-service pipelines was applied to the Fujian–Guangdong branch of the West–East Gas Pipeline III to verify its accuracy and feasibility. The research results offer technical support for the maintenance and emergency repair of pipeline leakage scenarios, leveraging intelligent pipeline technology to reduce costs and increase the efficiency of pipeline operations, thereby supporting the sustainable development of China's oil and gas pipelines with theoretical and technical backing.

Keywords: IoT technology; finite element simulation; neural algorithm prediction; negative pressure wave detection; self-rescue time simulation

Citation: Zhang, X.; Xie, X. Model for the Failure Prediction Mechanism of In-Service Pipelines Based on IoT Technology. *Processes* **2024**, *12*, 1642. https://doi.org/10.3390/pr12081642

Academic Editor: Marco Rossi

Received: 4 June 2024
Revised: 13 July 2024
Accepted: 13 July 2024
Published: 4 August 2024

1. Introduction

According to the medium-long-term Oil and Gas Pipeline Network Plan jointly issued by the National Development and Reform Commission and Energy Bureau, the mileage of China's oil and gas pipeline network will increase from 12×10^4 km to 24×10^4 km by 2025 [1], which puts forward higher requirements for the essential safety of pipe network construction and operation. Pipeline safety is an urgent issue that must be addressed. As most of the oil and gas pipelines in our country have entered the middle and later stages of service, aging problems are likely to occur one after another in the long-term operation of in-service pipelines, such as corrosion, corrosion defects, cracks, crack propagation, etc. [2]. How to slow down the pipeline corrosion rate, predict and identify pipeline corrosion in a timely and accurate manner, and ensure the safe transportation of oil and gas has become an urgent question in ensuring the safe operation of pipelines.

By 2023, the total mileage of China's long-distance natural gas pipelines was 11.8×10^4 km, and the annual gas volume was approximately 1500×10^8 m^3. With an increase in service time, pipelines exhibit defects such as corrosion, dents, cracks, and wrinkles. Statistics on the causes of pipeline failure in China in recent years show that corrosion-caused pipeline failure accounts for 20% of the total and is the primary mechanism of pipeline failure. Gong and Zhou [3] investigated the principle of corrosion pipeline failure and proposed that corrosion leads to the local thinning of the pipe wall; when the remaining wall thickness cannot bear the pipeline operating pressure, it leads to pipeline corrosion and defective area bursts, resulting in pipeline leakage. In addition, finite element analysis was applied to the study of corroded pipelines. Ahammed [4] and Qin [5] studied the factors that affect pipeline failure using finite element simulations and analyzed the influence of different sensitive parameters on pipeline failure pressure. Cui Mingwei and Cao Xuewen et al. [6], Chen-Liang et al. [7], Jian et al. [8], and Xuelui et al. [9] studied medium- and high-strength steel pipelines with corrosion defects. A failure pressure prediction formula was obtained by finite element simulation, and the accuracy of the failure pressure calculated by the fitting prediction formula was verified. Qin et al. [10], Jiali et al. [11], and Yue et al. [12] studied multipoint or overlapping corrosion in different pipeline transportation environments and developed a shadow response coefficient for different defects. The changes in the failure mode and stress distribution were studied to adapt to the failure pressure formula of pipelines with multiple corrosion defects. The design results can be used to predict and evaluate the residual strength of pipelines with multipoint corrosion defects.

Domestic pipeline leakage detection relies primarily on manual inspections and essential node detection methods, which cannot be performed in real time and cannot spontaneously detect instantaneous leaks or small leakage volumes. With the development of new-generation information technologies, such as IoT, big data, cloud computing, and artificial intelligence, the digital construction of pipeline networks is continuously advancing, and IoT technology is increasingly being applied [13]. Against this backdrop, IoT technology provides new ideas and methods for addressing pipeline leakage detection issues. IoT technology can provide intelligent methods for the safety management of oil and gas pipelines [14] and is the key to establishing a comprehensive lifecycle database and building precise algorithmic mechanism models [15]. As IoT technology is still under development, domestic research mainly focuses on data visualization, lacks support for algorithmic mechanism models, and has yet to effectively realize intelligence. Therefore, this study combines finite element model analysis and neural network learning algorithms to collect parameters related to the ultimate burst pressure of pipeline sections with corrosion defects to build an IoT-based pipeline failure pressure prediction framework and to integrate multi-source monitoring databases for corroded sections. The goal is to achieve the precise perception and prediction of a pipeline's status along its length, which is of great significance for the development of IoT technology and assessing the integrity of pipeline sections with corrosion defects.

2. Mechanism Model Construction

The construction of an in-service pipeline failure prediction mechanism model based on IoT technology involved four main steps. (1) Ultrasonic phased array technology was used to detect pipeline corrosion defects. By controlling the number and delay time of the excitation elements, the focus position of the ultrasonic waves and shift direction were controlled to detect the locations of various corrosion defects. A data-acquisition platform was set up to obtain further details about the defect sizes in combination with a phased array host. (2) A finite element model of the pipeline, considering the corrosion defects, was established. This model integrated the complete lifecycle data of a pipeline's design, construction, and operation, as well as multi-source monitoring data, such as pipeline stress and strain, the characteristics of pipeline materials, the diameter, wall thickness, and corrosion defect features, which were extracted to achieve a three-dimensional digital reconstruction of the pipeline. Considering operational loads such as the internal pressure and temperature along the pipeline, a pipeline stress–strain calculation model under different influencing factors was established using the domestic finite element analysis software Simdroid. (3) In addition, neural networks were used to predict the failure mechanics of corroded pipelines. The variable parameter ranges of the factors influencing the ultimate burst pressure of the pipeline were clarified. A single-parameter variable analysis was conducted using a finite element analysis model. The pipeline failure influencing factors and a stress–strain database were established using Simdroid 5.0, MATLAB 2021, and a pipeline failure mechanics prediction model was built using neural network algorithms. (4) Negative-pressure wave pipeline leakage detection technology was employed. Negative-pressure wave sensors were installed at both ends of the pressure pipeline. Suppose the pipeline reaches the burst pressure, causing a leakage incident. In this case, the instantaneous pressure drop is propagated along the pipeline, and a negative pressure is detected to determine the leakage location, flow, and other specific parameters. An alarm system is triggered, and the data collected by the sensors are uploaded to a remote control terminal. The TGNET software simulates the linear relationship between the pipeline operational parameters and failure time, thereby obtaining the pipeline's accident self-rescue time and providing rescue assurance for the pipeline's emergency maintenance.

2.1. Detection of Corrosion Defect Sizes in Pipelines Using Ultrasonic Phased Array Technology

Some problems with pipeline corrosion, such as solid concealment, are not easy to monitor in time. To directly show the pipeline morphology, defect volume, and spatial distribution in the corrosion area, a 3D model reconstruction method for an inner wall corrosion pipeline based on ultrasonic phased array technology was proposed [16]. Ultrasonic phased array technology is based on phased array radar technology and uses several array element wafers that can independently emit ultrasonic beams, and the number and delay time of the excitation element wafers are controlled by electronic technology. The focusing position and deflection direction of the ultrasonic beam can be controlled [17,18]. When ultrasonic phased array technology is used to detect inner wall corrosion in pipelines, a one-dimensional linear array probe is placed on the outer wall of the pipeline, perpendicular to it, and ultrasonic waves are emitted inward along the surface. The ultrasonic wave emitted by the probe is reflected through the inner wall of the pipeline and received by the probe to produce an interface-reflected wave. The above process is repeated, and the pipe wall thickness can be calculated using the difference between the times the reflected wave touches the inner and outer walls of the pipeline. Thus, the location of the corrosion defect can be detected [19].

When using ultrasonic phased array technology to inspect corroded pipes on the inner wall, a one-dimensional linear array probe is placed on the outer wall of the pipe, perpendicular to it, and it emits ultrasonic waves inward along the surface (as shown in Figure 1, where T is the time and W is the beam value of the sound wave). The ultrasonic wave emitted by the probe is reflected through the inner wall of the pipeline for the first time and is received by the probe, generating an interfacial reflected wave A. The ultrasonic wave is reflected through the inner wall of the pipeline for a second time and is received by the probe to produce a secondary interfacial reflected wave B, and so on, to form three echoes C, four echoes D, and so on. During the scanning process, the probe is employed four times, at T1–T4, where T1 and T4 represent the times of the detection of ultrasonic waves at the outer wall of the pipeline, and T2 and T3 represent the times of the detection of ultrasonic waves at the inner wall of the pipeline. The difference between the times when the reflected waves touch the inner and outer walls of the pipe can be used to calculate the wall thickness of the pipe and detect the location of corrosion defects.

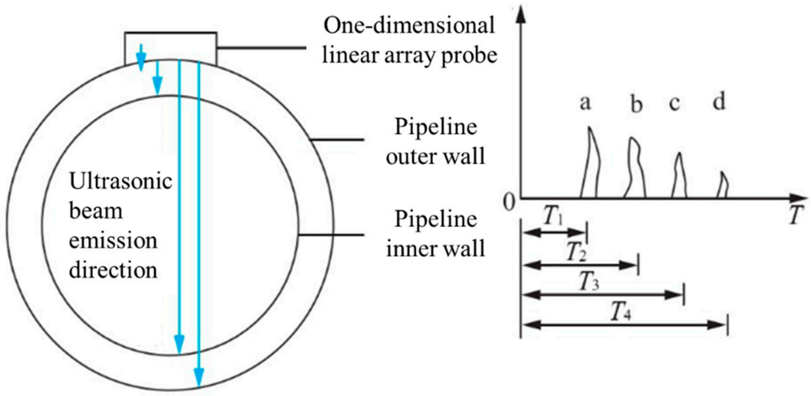

Figure 1. Schematic of ultrasonic phased array detection method for corroded pipelines [6].

A self-developed acquisition platform was used to control the ultrasonic phased array one-dimensional linear array probe, which preliminarily determined the location of pipeline corrosion defects. The spatial coordinates of the internal and external diameters of the corroded pipeline were detected using the reflected echo signals, and an interpolation algorithm was applied to generate a point cloud dataset for the internal and external diameters. Layered scanning methods were employed to acquire point-cloud data at various levels. The collected point-cloud data were then reconstructed into a three-dimensional model using reverse and forward modeling methods, and the accuracy of the scan data was enhanced by comparing it with data obtained from a 3D laser scanner.

2.2. Establishment of a Finite Element Model for Pipelines with Corrosion Defects

For a pipeline with corrosion defects detected by the ultrasonic phased array testing method, to more accurately and correctly judge the failure pressure of the pipeline, combined with its specific defect parameters, a finite element numerical simulation stress analysis of the pipeline with corrosion defects was conducted using Simdroid simulation software.

2.2.1. Finite Element Model Material

The material of the buried long-distance pipeline is X70 steel; the outer diameter of the pipeline is 1219 mm; its wall thickness is 19.89 mm; its elastic modulus is 210 GPa; its Poisson's ratio is 0.3; its yield stress is 641 MPa; and the depth at which it is buried is 1 m. The stress–strain change in the pipe using the Ramberg–Osgood constitutive equation is shown in Figure 2, and the stress–strain relationship is expressed by Formula (1).

$$\varepsilon = \frac{\sigma}{E} + \alpha \frac{\sigma}{E}\left(\frac{\sigma}{\sigma_Y}\right)^{n-1} \tag{1}$$

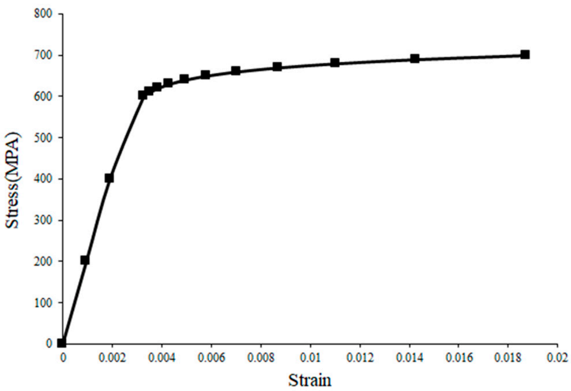

Figure 2. Diagram of stress–strain curves of pipe materials.

2.2.2. Corrosion Defect Model

As different defects exist in the pipeline, such as pits and local thinning caused by corrosion, a rectangular defect was used to simplify the modeling of the thinning position of the pipeline. The dimensionless variables in the finite element model took into account the influence of different clothing parameters on the pipeline impact. For the pipeline defect parameters, the corrosion length was set to K_l, the corrosion depth to K_d, and the corrosion width to K_w. Each parameter is determined by Formula (2). The influence of the corrosion volume parameters on the pipeline failure pressure was studied using these parameters.

$$\begin{cases} K_l = L/\sqrt{Dt} \\ K_d = d/t \\ K_w = \beta/360^\circ \end{cases} \tag{2}$$

2.2.3. Load and Boundary Conditions

In this model, only the internal pressure of the pipe was considered. The internal pressure load was applied monotonously to the inner wall, and the loading direction of the internal pressure was perpendicular to the inner wall of the pipeline, indicating that the pipeline was closed. The pressure end load was loaded into the unconstrained end of the model and was determined using Formula (3).

$$P = \frac{P_0 D}{4t} \tag{3}$$

The defects in the corroded pipes are shown in Figure 3. The initial stress of the pipeline was set as follows: The initial stress of the pipeline was determined by applying the processing load (internal pressure, temperature, etc.) to mimic the actual situation. Furthermore, to prevent the axial displacement of the pipeline, an axial constraint was applied to the interface of the intact pipeline, and a symmetrical constraint was imposed on both ends of the cross-section of the pipeline defect [10].

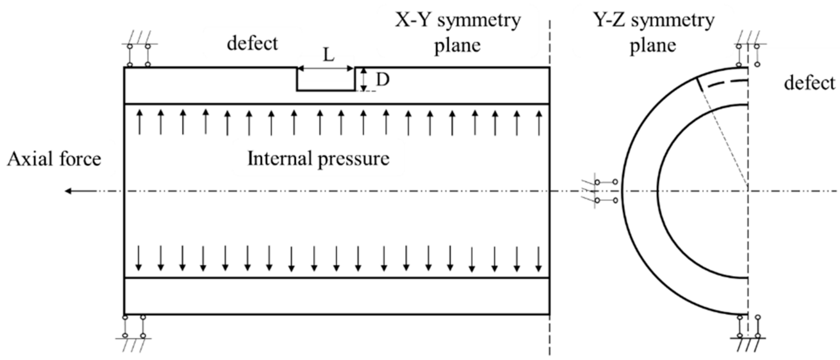

Figure 3. Schematic of corroded pipeline defects.

2.2.4. Failure Criterion

To determine the limit blasting pressure of a corroded pipeline, the commonly used failure criteria are the stress, strain, and numerical instability [20]. Many prototype experiments and numerical simulations have shown that the stress failure criterion yields high accuracy when calculating the ultimate blasting pressure of a corroded pipeline; therefore, the stress failure criterion was adopted in this study. It is considered that when the stress state of the corrosion region reaches the endpoint of the post-yield strengthening stage, that is, when the minimum von Mises equivalent stress in the corrosion zone reaches the tensile strength of the material, the pipeline experiences plastic failure. Otherwise, it is safe. Then, the blasting pressure applied to the pipeline is the failure pressure of the pipeline; that is,

$$\sigma_M = \sqrt{\left[(\sigma_1-\sigma_2)^2+(\sigma_2-\sigma_3)^2+(\sigma_3-\sigma_1)^2\right]/2} \le \sigma_u \tag{4}$$

2.2.5. Model Verification

An example verification of a pipeline with a single corrosion defect was carried out according to the blasting experiment of corroded steel pipes by Benjamin [21] of PETROBRAS. We selected the experimental condition IDTS2 to verify the finite element model in this study. Table 1 lists the failure pressure predicted by the finite element model, Pf, and the failure pressure measured during the test, Pexp. The error between the predicted and measured values was approximately 2.29%. A comparison of the local fracture and failure behaviors is shown in Figure 4. The failure mode determined by the finite element model was similar to the behavior observed in the test, which verifies the correctness of the finite element model.

Table 1. Comparison between the finite element model results and the measured failure pressure.

Working Condition	Pexp/MPa	Pf/MPa	Error/%
IDTS 2	22.68	23.20	2.29

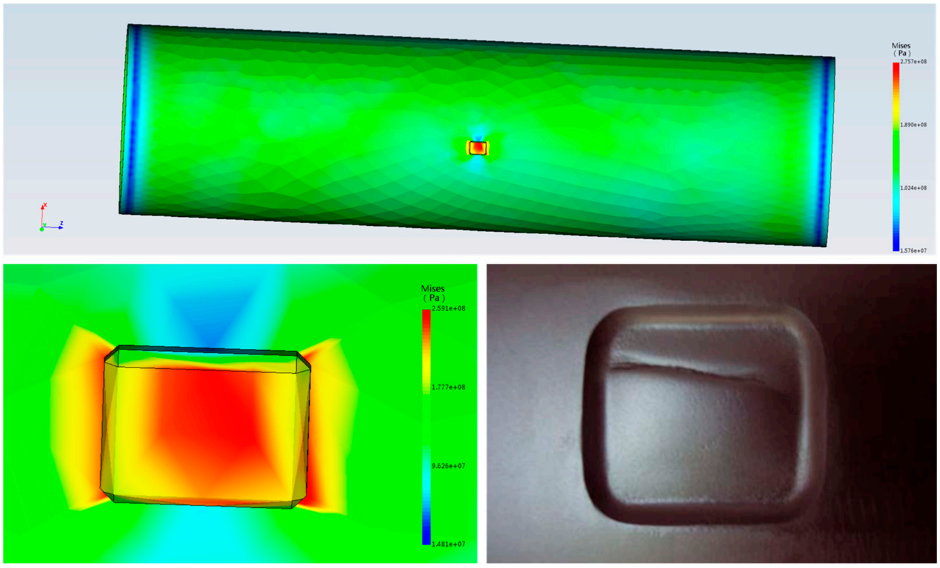

Figure 4. Comparison of test and numerical simulation results under test conditions.

2.3. Pipeline Failure Mechanics Prediction Model Based on Neural Networks

A pipeline model with corrosion defects was established based on the actual working condition data. The failure of a pipeline with corrosion defects was determined using a simulation model, and the stress distribution cloud diagram of the pipeline model is shown as Figure 4. The ultimate blasting pressure of the pipeline was determined. The key factors affecting the failure pressure of a pipeline with corrosion defects are divided into the following two types: The working condition parameters of the pipeline, such as the internal pressure and operating temperature, have a significant impact on the stress state distribution of the pipeline. Defect size parameters, such as the defect length, width, depth, and defect-related characteristic parameters, determine the displacement load form in the finite element model and the stress distribution along the pipeline [22]. Based on the actual operating conditions, a single-variable analysis of the variable influence parameters was carried out. The results of this analysis, combined with the output results of the finite element model, were used to analyze the influence of different parameters on the ultimate blasting pressure of the pipeline. The output results were fed into a neural network for learning, and the pipeline failure pressure was predicted. The BP neural network has the advantages of good self-learning and robustness and can better deal with pipeline failure prediction problems with less historical data and nonlinear failures [23].

Based on the characteristics of the safety state prediction of corrosion-defective pipelines and the data calculated using the finite element model, the ultimate blasting pressure was predicted using the regression model of the neural network. The algorithm [24] was implemented using MATLAB 2021, and the specific construction flowchart is shown in Figure 5. The construction process is mainly divided into four steps [25]: (1) The data are read; the first five columns (pipe diameter, wall thickness, defect depth, defect length measurement, and defect width measurement) are taken as the features of the model and the last column as the target value; and the features and target value are normalized. (2) The data are divided into training and verification sets, and the features and target values are divided into training and verification sets. (3) A neural network model is created with a specified number of neurons in the hidden layer. When setting the training parameters, the code specifies the number of training rounds, learning rate, minimum gradient, and other parameters. (4) The neural network model is trained using the characteristics and target values of the training set as input. After the completion of the training, the model was used to predict the characteristics of the verification set and generate the limit blasting pressure labels.

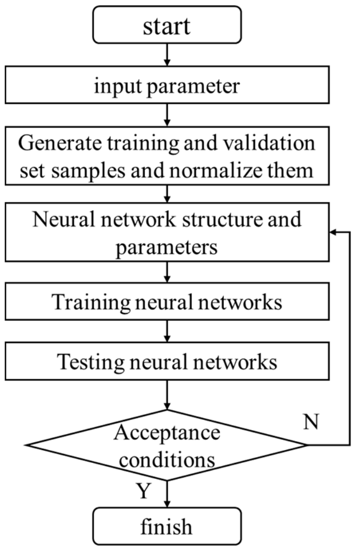

Figure 5. BP neural network construction flowchart.

2.3.1. Acquisition and Analysis of Pipeline State Data

In this study, the finite element analysis method with the highest reliability was selected to study the influence of the corrosion volume parameters on the pipeline failure pressure to accurately and efficiently evaluate the residual strength of the pipeline. For the calculation results, considering the changes in various corrosion volume parameters, 173 datasets [26] were selected for training the model.

2.3.2. Establishment of BP Neural Network Model

Based on the characteristics of the safety state prediction of pipelines with corrosion defects and the data calculated using the finite element model, the ultimate blasting pressure was predicted using the regression model of the neural network. The algorithm is implemented in MATLAB [27]. The specific process is as follows:

1. The data from the Excel file were read using the misread function; the first five columns were considered the features (pipe diameter, wall thickness, defect depth measurement, defect length measurement, and defect width measurement), and the last column was considered the target value of the model. The score function was then used to normalize the features and target values.
2. The proportion of data to be divided into training and verification sets was determined by defining the split_ratio, and the features and target values were divided into the training and verification sets based on this ratio.

3. A fitness function was used to create a neural network model with a specified number of neurons in the hidden layer. In setting the training parameters, the code specified parameters such as the number of training wheels, learning rate, and minimum gradient.
4. The training function was called to train the neural network model, and the characteristics and target values of the training set were used as the input. After the training was completed, the model was used to predict the characteristics of the verification set, and the predicted limit blasting pressure labels were generated.
5. If the input data were normalized, the code would also normalize the predicted results and target values of the validation set.
6. The predicted limit blasting pressure values were sorted, and the fitting curve between the actual and predicted values was plotted. Table 7 shows the relationship between the predicted and actual values used to evaluate the fitting effect of the model.

2.3.3. Model Running Result Display

The code was run in MATLAB. The data were split; the first 80% of the data were used for training, and the 20% of pipe-related running parameters were used for verification. The results are shown in Figure 6.

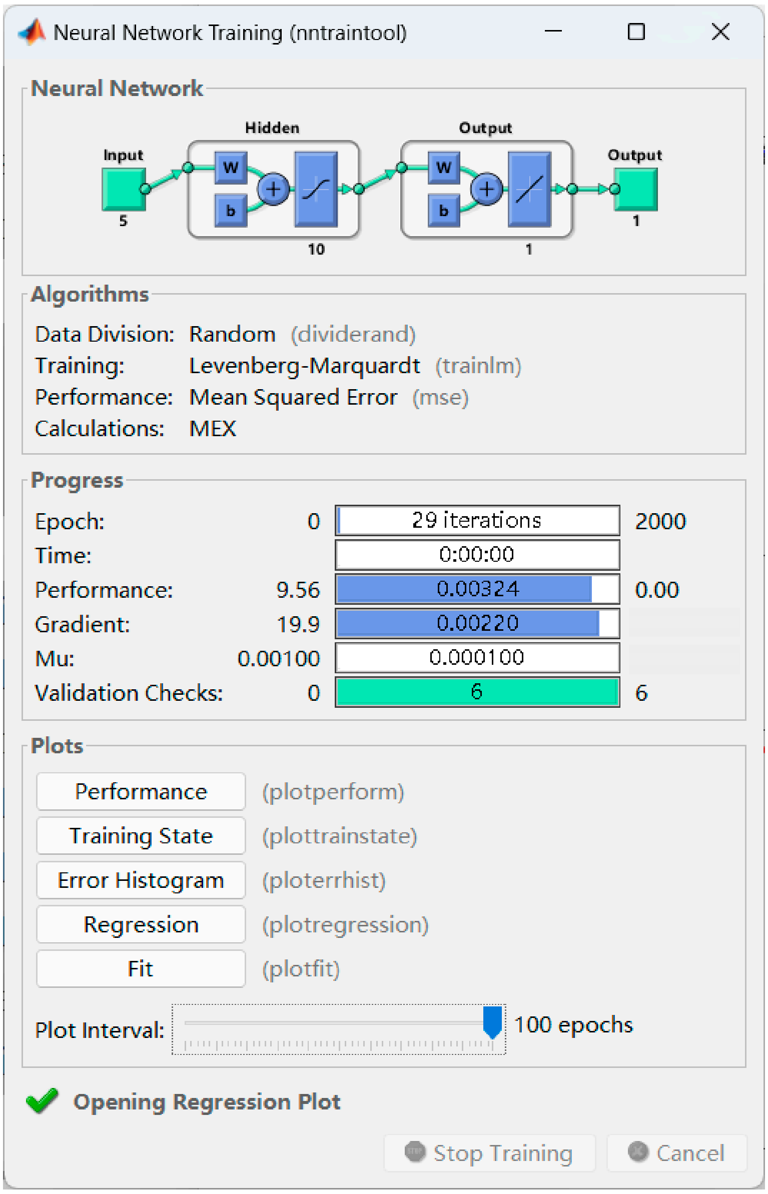

Figure 6. Neural network training diagram.

An example analysis was conducted, and a comparison of the sample values with the predicted values is shown in Figure 7. It was shown that the BP neural network can better deal with the safety state prediction of a single corrosion defect pipeline and yield a more accurate failure state value, which can be used as a reference for pipeline preventive inspection and time series analysis. This study provides a theoretical basis for a feasible pipeline preventive maintenance protocol.

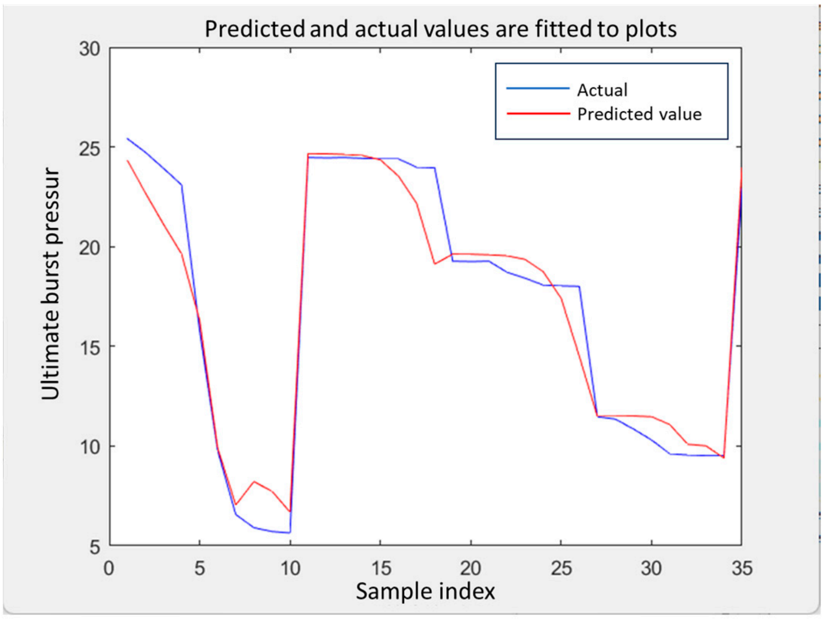

Figure 7. Comparison of the actual and predicted values of the sample.

2.4. Leak Detection and Self-Rescue Time Prediction

When the operating pressure at the corrosion defect site of the pipeline reaches the failure pressure predicted by the neural network, the pipeline is at a high risk of bursting, leading to leakage. When a leak occurs, the high pressure inside the pipeline compared to the atmospheric pressure outside causes the fluid to escape rapidly, resulting in a pressure drop at the leakage point [28]. Owing to the continuity of the fluid flow near the leak point, the pipeline flow rate remains almost constant. However, a pressure difference exists between the leak point and adjacent areas, causing the high-pressure fluid at the leak point to flow into the low-pressure area, resulting in the spread of the leak along the pipeline, both upstream and downstream. This pressure-change phenomenon, which is caused by a leak, is called a negative pressure wave. As shown in Figure 8, by installing pressure sensors at both ends of the pipeline, the transient negative pressure wave during the leakage process can be monitored in real time to locate the leak point [29]. Once a pipeline leak is detected and a leak monitoring alarm is triggered, immediate pipeline repair must commence. The TGNET software was used to simulate the pipeline pressure drop trend using the instantaneous data collected by the data acquisition station. By simulating and analyzing parameters such as the flow rate, pressure, and temperature at the leakage point, the self-rescue time range of the pipeline under leakage conditions can be determined [30], which can indicate that urgent pipeline repair work is required.

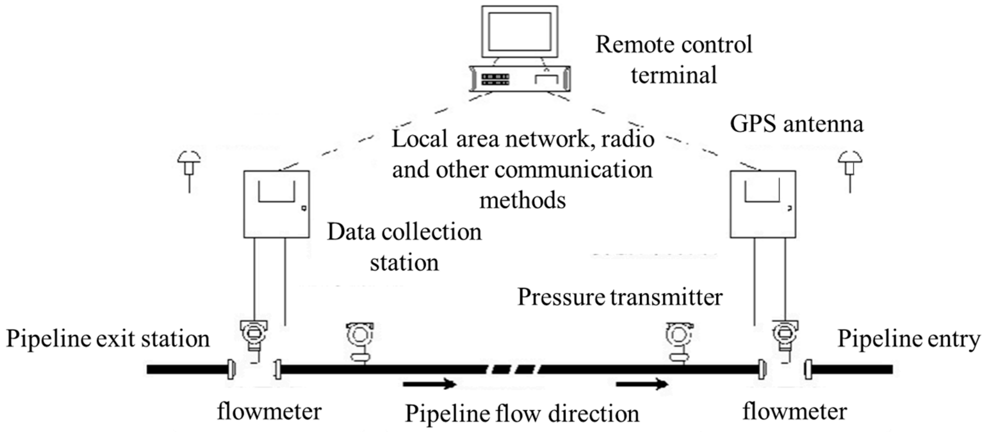

Figure 8. Schematic of negative pressure wave sensing.

3. Case Verification

The verification of the proposed model was conducted using the Fujian–Guangdong branch of the West–East Gas Pipeline Project Line 3 as an example. The pipeline of this project is 192 km long, with a steel grade of X70, yield strength of 485 MPa, diameter of 813 mm, and designed gas transmission capacity of 5.7×10^9 m^3/a. The pipeline traverses diverse topographies, mainly low hills with undulating terrain and predominantly forest orchard land. Line 3 of the West–East Gas Pipeline Project operates in a warm and humid environment, rendering the pipeline susceptible to corrosion [31]. First, ultrasonic phased array technology was used to detect pipeline corrosion. The position and size of the corrosion defects within a 100 m section of the pipeline were determined, and the specific data collection points are shown in Figure 9.

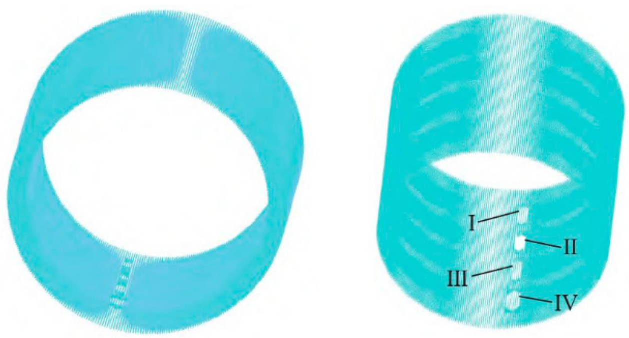

Figure 9. Raw point cloud data acquisition map of the corroded pipeline.

Using the actual field data and the parameters of the pipeline, such as its material (X70 steel) and diameter, a finite element model of the pipeline with corrosion defects was established using Simdroid, as shown in Figure 10. As the pipeline had various types of defects at different points, the minimum pressure obtained from the different defect simulations was selected as the overall segment failure pressure.

According to the finite element model analysis, the factors affecting the failure of a pipeline with corrosion defects, ordered in terms of sensitivity, are the corrosion defect length, corrosion defect depth, corrosion defect width, wall thickness, pipeline diameter, and operating pressure. The defect parameters significantly affect the ultimate burst pressure of the pipeline. Therefore, the defect length, width, and depth were selected as the key parameters affecting pipeline failure pressure, and their reliability ranges were defined. Single-variable analysis was performed in combination with the finite element model. Sixty-two datasets were cumulatively generated for prediction and verification by a neural network. The specific data are presented in Table 2. In addition, the 173 datasets used for the finite element model simulations in [24] were selected as the neural network prediction training set to generate the neural network prediction target pipeline failure pressure database.

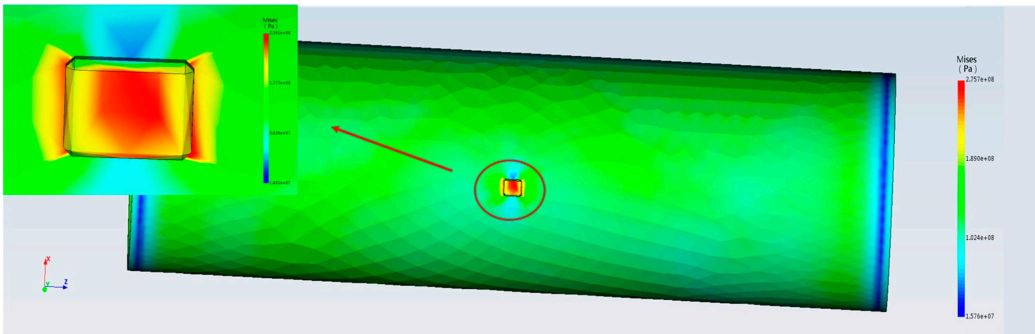

Figure 10. Finite element model diagram of a pipe with corrosion defects.

After normalizing the input data, splitting the data, setting the training parameters, training the model, and visualizing the prediction results, the algorithm for the model used for the quasi-combined prediction of limit blasting pressure was established, and the neural network fitting training regression is shown in Figure 11. The difference between the predictions of the neural network and the actual data was less than 10%, and the correlation coefficients of the prediction results of the Shenjing network were all greater than 0.99, indicating that the neural network could better deal with the safety state prediction questions of corrosion-defective pipelines and obtain accurate failure state values.

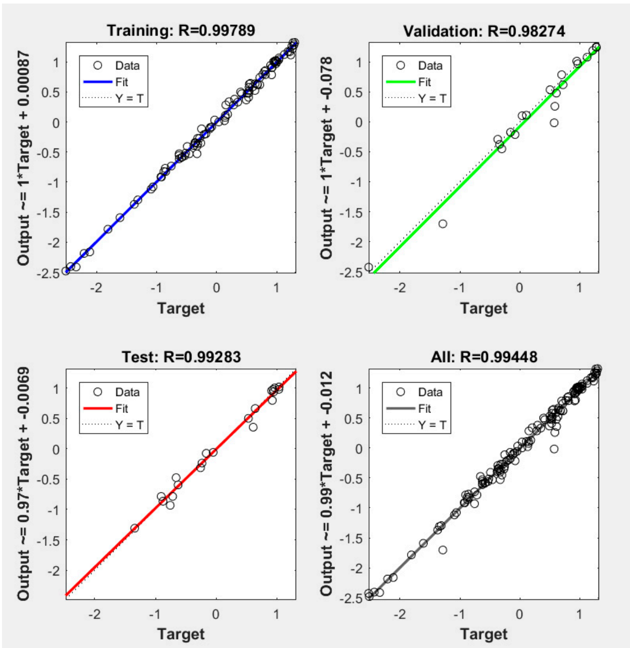

Figure 11. Neural network training regression graphs.

An analysis was conducted based on the operating conditions of the Fujian–Guangdong branch of the West–East Gas Pipeline Project Line 3. The real-time pipeline pressure changes were monitored using pressure transmitters at both ends of the pipeline. If the pipeline reached the ultimate burst pressure and resulted in leakage, a self-rescue time simulation was performed using TGNET software based on the leakage point conditions (temperature, pressure, flow rate, etc.). The pipeline pressure was simulated as an independent variable to obtain a linear relationship between the leakage pipeline pressure changes and the self-rescue time, as shown in Figure 12. Pipeline leakage self-rescue must be completed within a short period to provide a time margin for pipeline repair.

Table 2. Calculation results of different parameters and failure pressure.

No.	Pipe Diameter/mm	Wall Thickness/mm	Operating Pressure/MPa	K_l	K_d	K_w	Failure Pressure/MPa	No.	Pipe Diameter/mm	Wall Thickness/mm	Operating Pressure/MPa	K_l	K_d	K_w	Failure Pressure/MPa
1	965	19.89	10	4.0	0.8	0.083	6.71	32	1219	19.89	10	1.5	0.65	0.083	9.51
2	1219	19.89	10	4.0	0.8	0.083	6.26	33	1219	19.89	10	3.0	0.65	0.083	8.81
3	1422	19.89	10	4.0	0.8	0.083	6.19	34	1219	19.89	10	4.5	0.65	0.083	8.58
4	965	19.89	10	5.0	0.8	0.083	6.98	35	1219	19.89	10	6.0	0.65	0.083	8.33
5	1219	19.89	10	5.0	0.8	0.083	6.66	36	1219	19.89	10	1.5	0.45	0.083	11.99
6	1422	19.89	10	5.0	0.8	0.083	6.56	37	1219	19.89	10	3.0	0.45	0.083	11.24
7	965	19.89	10	6.0	0.8	0.083	7.42	38	1219	19.89	10	4.5	0.45	0.083	11.86
8	1219	19.89	10	6.0	0.8	0.083	7.06	39	1219	19.89	10	6.0	0.45	0.083	10.21
9	1422	19.89	10	6.0	0.8	0.083	7.03	40	1219	19.89	10	2.5	0.50	0.083	7.19
10	1219	17.50	8	4.0	0.8	0.083	7.63	41	1219	19.89	10	2.5	0.60	0.083	6.99
11	1219	19.89	8	4.0	0.8	0.083	7.37	42	1219	19.89	10	2.5	0.70	0.083	6.84
12	1219	22.20	8	4.0	0.8	0.083	7.20	43	1219	19.89	10	2.5	0.80	0.083	6.82
13	1219	17.50	10	4.0	0.8	0.083	7.32	44	1219	19.89	10	5.0	0.50	0.083	6.99
14	1219	19.89	10	4.0	0.8	0.083	7.05	45	1219	19.89	10	5.0	0.60	0.083	6.81
15	1219	22.20	10	4.0	0.8	0.083	6.93	46	1219	19.89	10	5.0	0.70	0.083	6.67
16	1219	17.50	12	4.0	0.8	0.083	7.26	47	1219	19.89	10	5.0	0.80	0.083	6.61
17	1219	19.89	12	4.0	0.8	0.083	6.98	48	1219	19.89	10	7.5	0.50	0.083	6.71
18	1219	22.20	12	4.0	0.8	0.083	6.81	49	1219	19.89	10	7.5	0.60	0.083	6.61
19	1219	19.89	8	4.0	0.8	0.083	7.37	50	1219	19.89	10	7.5	0.70	0.083	6.47
20	1219	19.89	10	4.0	0.8	0.083	7.05	51	1219	19.89	10	7.5	0.80	0.083	6.41
21	1219	19.89	12	4.0	0.8	0.083	6.97	52	1219	19.89	10	2.5	0.45	0.06	9.35
22	1219	19.89	8	5.0	0.8	0.083	7.09	53	1219	19.89	10	2.5	0.45	0.11	11.08
23	1219	19.89	10	5.0	0.8	0.083	6.92	54	1219	19.89	10	2.5	0.45	0.17	12.85
24	1219	19.89	12	5.0	0.8	0.083	6.79	55	1219	19.89	10	2.5	0.45	0.22	13.64
25	1219	19.89	8	6.0	0.8	0.083	7.23	56	1219	19.89	10	5.0	0.45	0.06	9.17
26	1219	19.89	10	6.0	0.8	0.083	7.05	57	1219	19.89	10	5.0	0.45	0.11	10.92
27	1219	19.89	12	6.0	0.8	0.083	6.09	58	1219	19.89	10	5.0	0.45	0.17	12.73
28	1219	19.89	8	4.0	0.8	0.083	7.37	59	1219	19.89	10	5.0	0.45	0.22	12.88
29	1219	19.89	10	3.0	0.85	0.083	6.98	60	1219	19.89	10	7.5	0.45	0.06	9.12
30	1219	19.89	10	4.5	0.85	0.083	6.85	61	1219	19.89	10	7.5	0.45	0.11	9.83
31	1219	19.89	10	6.0	0.85	0.083	6.73	62	1219	19.89	10	7.5	0.45	0.17	11.12

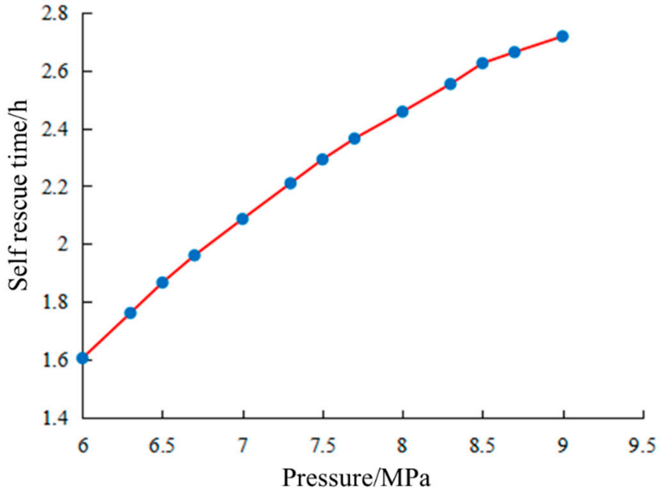

Figure 12. Fitting curve of the relationship between leakage pipeline pressure and self-rescue time.

The relationship between the self-rescue time y and leakage pipeline pressure x was obtained using curve fitting. An R^2 value of 0.998 was obtained, showing a good fit. The expression for the fitting curve is given below.

$$y == -0.0068x^4 + 0.2004x^3 - 2.2696x^2 + 12.0029x - 23.2397 \quad (5)$$

4. Conclusions

The rapid development of new-generation intelligent pipeline technology has gradually led to digitalized operations, informationalized management, and visualized processes in pipeline construction and operation. Intelligent pipeline technology addresses the shortcomings of traditional management methods. The surge in the use of intelligent technology and the rapid development of the Internet of Things, big data, and artificial intelligence present new avenues for addressing the challenges in oil and gas pipeline management.

In this study, a corroded pipeline section was selected as the research object. The overall mechanism model combined with IoT technology uses ultrasonic phased array technology to determine the location of corrosion defects and obtain accurate defect size parameters (length, depth, and width) through data processing. The defect parameters, along with Simdroid domestic finite element software, were used to analyze the stress and strain state parameters of the pipeline. Single-variable analysis was conducted within the selected variable parameter range to generate a finite element model dataset. A finite element database was integrated using a neural network model to predict the ultimate burst pressure of a corroded pipeline. A negative-pressure wave-sensing system monitors the operating pressure in real time, triggering an alarm if the pressure approaches the neural-network-predicted burst pressure value. Instantaneous pipeline operation data were uploaded to a remote control terminal for self-rescue time prediction, providing pipeline maintenance and repair time estimates. This preliminary exploration of intelligent development directions for in-service pipeline safety measures based on IoT technology offers new ideas and methods for managing the safety of in-service pipelines in China and provides theoretical and technical support for the digital lifecycle management of pipelines.

Author Contributions: Conceptualization, X.Z.; methodology, X.Z.; software, X.Z.; validation, X.Z.; formal analysis, X.Z.; investigation, X.Z.; resources, X.X.; data curation, X.Z.; writing—original draft preparation, X.Z.; writing—review and editing, X.X.; visualization, X.X.; supervision, X.X.; project administration, X.X.; and funding acquisition, X.X. All authors have read and agreed to the published version of the manuscript.

Funding: This research was funded by the China Petroleum Science and Technology Innovation Fund (grant number 2017D-5007-0606).

Data Availability Statement: The original contributions presented in the study are included in the article, further inquiries can be directed to the corresponding author.

Conflicts of Interest: The authors declare no conflicts of interest.

References

1. Huang, W.H. Interpretation and Reflections on China's Medium- and Long-Term Oil and Gas Pipeline Network Planning. *Sci. Chin.* **2017**, *27*, 64–65.
2. Che, C.Y. Study on Failure Risk and Early Warning of Corroded Subseaoil and Gas Pipeline Based on Time-Varying Reliability. Master's Thesis, Xi'an University of Architecture and Technology, Xi'an, China, 2019.
3. Gong, C.; Zhou, W. First-order reliability method-based system reliability analyses of corroding pipelines considering multiple defects and failure modes. *Struct. Infrastruct. Eng.* **2017**, *13*, 1451–1461. [CrossRef]
4. MAhammed, R.E. Melchers. Reliability estimation of pressurized pipelines subject to localized corrosion defects. *Int. J. Press. Vessel. Pip.* **1996**, *69*, 267–272. [CrossRef]
5. Qin, G.; Huang, Y.; Wang, Y.; Cheng, Y.F. Pipeline condition assessment and finite element modeling of mechano-electrochemical interaction between corrosion defects with varied orientations on pipelines. *Tunn. Undergr. Space Technol.* **2023**, *136*, 105101. [CrossRef]
6. Cui, M.W.; Cao, X.W. Effect of corrosion defects on failure pressure of medium and high strength oil and gas pipelines. *Acta Pet. Sin.* **2012**, *33*, 1086–1092.
7. Su, C.-L.; Li, X.; Zhou, J. Failure pressure analysis of corroded moderate-to-high strength pipelines. *China Ocean. Eng.* **2016**, *30*. [CrossRef]
8. Shuai, J.; Zhang, C.E.; Chen, F.L. Nonlinear finite element method for failure pressure prediction of corroded pipelines. *Acta Pet. Sin.* **2008**, *29*, 933–937.
9. Zang, X.R.; Gu, X.T.; Wang, Q.Y.; Wang, L.H. Failure pressure model of high-steel grade gas pipeline with corrosion defects. *Oil Gas Storage Transp.* **2019**, *38*, 285–290+296.
10. Qin, P.C.; Xiong, C.B.; Li, Z.; Zhai, J.S. Failure pressure analysis of submarine pipeline considering the effect of multiple corrosion defects. *Surf. Technol.* **2020**, *49*, 237–244.
11. Wu, J.L. X80 Pipe Failure Analysis with Corrosion Defects. Master's Thesis, Southwest Petroleum University, Nanchong, China, 2018.
12. Zhang, Y. Study on residual strength of multi-point corrosion defect pipeline based on finite element and PSO-BP. Master's Thesis, Xi'an University of Architecture and Technology, Xi'an, China, 2020.
13. Sun, C.J. Discussion on Information Security Protection Strategies for the Perception Layer of the Internet of Things. *Commun. World* **2019**, *26*, 1–2.
14. Anshi Asia Pacific Digital Twin Laboratory White Paper on Digital Twin Technology. [R/OL] (2019-2012-20) [2021-07-10].
15. Sridhar, S.; Smys, S. Intelligent security framework for iot devices cryptography based end-to-end security architecture. In Proceedings of the International Conference on Inventive Systems & Control, Coimbatore, India, 19–20 January 2017.
16. Zhang, Y.L.; Hou, R.G.; Wang, R.; Zhang, M.M.; Lv, Z. Reconstruction of three-dimensional models of inner wall corroded pipelines based on ultrasonic phased array technology. *Oil Gas Storage Transp.* **2023**, *42*, 1369–1375.
17. Li, Y.X.; Wang, X.K.; Dong, X.Y.; Guan, S.Y. Ultrasonic phased array detection technology for forming defects in wheel hub bearing raceways. *J. Plast. Eng.* **2022**, *29*, 61–66. [CrossRef]
18. Cao, Y.L.; Yun, W.R. Appication of ultrasonic phased array multi focus technique in austentic stainless steel testing. *J Nondestouctive Test. Technol.* **2022**, *46*, 43–45.
19. Liang, G.A.; Yao, Y.Z.; Zheng, K.; Xu, Q.; Wang, H.L.; Wang, H.T. Research on signal reconstruction method for corner weld defects based on ultrasonic phased array. *Comput. Meas. Control.* **2022**, *30*, 222–228. [CrossRef]
20. Sun, M.M.; Fang, H.Y.; Zhao, H.S.; Li, X. Influencing factors and evaluation methods of failure pressure of irregular defective pipelines. *J. China Univ. Pet. (Nat. Sci. Ed.)* **2022**, *46*, 152–159.
21. Benjamin, A.C.; Freire, J.L.F.; Vieira, R.D.; Diniz, J.L.C.; de Andrade, E.Q. Burst Tests on Pipeline Containing Interacting Corrosion Defects. In Proceedings of the ASME 2005 24th International Conference on Offshore Mechanics and Arctic Engineering, Halkidiki, Greece, 12–17 June 2005; Volume 3, pp. 403–417. [CrossRef]
22. Chen, R.M.; Qiu, J.S.; Liu, B.Y.; Reng, G.L. Research on residual strength of corroded pressure pipelines based on burst failure. *Ship Mech.* **2020**, *24*, 925–933.
23. Qi, F.; Gan, B.; Cheng, T.L.; Ma, W.F.; Yao, T.; Wang, K. Failure prediction and sensitivity analysis of pipeline circumferential welds based on neural networks. *J. Southwest Univ. (Nat. Sci. Ed.)* **2024**, *46*, 159–167. [CrossRef]
24. Guoh, L. Research on Residual Strength Evaluation Method of X80 Natural Gas Pipeline with Rectangular Uniform Wall Thickness Corrosion Defect. Master's Thesis, Chongqing University of Science and Technology, Chongqing, China, 2021. [CrossRef]
25. Guo, D.; Zhou, J. Research on neural network prediction model based on MATLAB. *Logist. Sci. Technol.* **2006**, 125–128.
26. Wang, Y.; Jia, S.Q.; Li, N.W.; Guo, T. Research on Neural Network Method for Predicting Burst Pressure of Oil and Gas Pipelines with Defects. *Green Technol.* **2023**, *25*, 111–115. [CrossRef]

27. Jia, S.Q.; Qie, Y.H.; Li, Y.T.; Li, N.N. Research on prediction of explosion pressure in oil and gas pipelines with uniform corrosion defects based on genetic neural network algorithm. *China Saf. Prod. Sci. Technol.* **2020**, *16*, 105–110.
28. Yao, D.N. Simulation Study on Pressure Fluctuation Characteristics of Fluid Pipeline Leakage. Master's Thesis, Northeast University of Petroleum, Daqing, China, 2020. [CrossRef]
29. Ma, X.J.; Dang, Y.H.; Xu, J.T.; Yang, J.; Wen, H. The Application of Pipeline Leakage Online Monitoring System in Oil Pipeline. *Electron. World* **2020**, *6*, 179–180. [CrossRef]
30. Wang, S.M. Research on Operation and Dispatching Plan of Gas Pipeline Network in Southern Shanxi. Master's Thesis, China University of Petroleum (East China), Qingdao, China, 2024.
31. The West East Gas Pipeline Fuzhou Connection Line has been officially put into operation. *Pet. Eng. Constr.* **2020**, *46*, 40.